



Impaired cardiac branched-chain amino acid metabolism in a novel model of diabetic cardiomyopathy

Asakura, Junko ; Nagao, Manabu ; Shinohara, Masakazu ; Hosooka, Tetsuya ; Kuwahara, Naoya ; Nishimori, Makoto ; Tanaka, Hidekazu ; Satomi-...

(Citation)

Cardiovascular Diabetology, 24(1):167

(Issue Date)

2025-04-16

(Resource Type)

journal article

(Version)

Version of Record

(Rights)

© The Author(s) 2025.

This article is licensed under a Creative Commons Attribution-NonCommercial-NoDerivatives 4.0 International License, which permits any non-commercial use, sharing, distribution and reproduction in any medium or format, as long as you give...

(URL)

<https://hdl.handle.net/20.500.14094/0100495756>



METHODOLOGY

Open Access



Impaired cardiac branched-chain amino acid metabolism in a novel model of diabetic cardiomyopathy

Junko Asakura¹, Manabu Nagao^{2*}, Masakazu Shinohara^{3,4}, Tetsuya Hosooka^{5,6}, Naoya Kuwahara¹, Makoto Nishimori³, Hidekazu Tanaka¹, Seimi Satomi-Kobayashi¹, Sho Matsui⁷, Tsutomu Sasaki⁷, Tadahiro Kitamura⁸, Hiromasa Otake¹, Tatsuro Ishida^{1,9}, Wataru Ogawa⁶, Ken-Ichi Hirata^{1,2} and Ryuji Toh²

Abstract

Background Systemic insulin resistance plays an important role in the pathogenesis of type 2 diabetes and its complications. Although impaired branched-chain amino acid (BCAA) metabolism has been reported to be involved in the development of diabetes, the relationship between cardiac BCAA metabolism and the pathogenesis of diabetic cardiomyopathy (DbCM) remains unclear.

Objectives The aim of this study was to investigate BCAA metabolism in insulin-resistant hearts by using a novel mouse model of DbCM.

Methods The cardiac phenotypes of adipocyte-specific 3'-phosphoinositide-dependent kinase 1 (PDK1)-deficient (A-PDK1KO) mice were assessed by histological analysis and echocardiography. The metabolic characteristics and cardiac gene expression were determined by mass spectrometry or RNA sequencing, respectively. Cardiac protein expression was evaluated by Western blot analysis.

Results A-PDK1KO mouse hearts exhibited hypertrophy with prominent insulin resistance, consistent with cardiac phenotypes and metabolic disturbances previously reported as DbCM characteristics. RNA sequencing revealed the activation of BCAA uptake in diabetic hearts. In addition, the key enzymes involved in cardiac BCAA catabolism were downregulated at the protein level in A-PDK1KO mice, leading to the accumulation of BCAAs in the heart. Mechanistically, the accumulation of the BCAA leucine caused cardiac hypertrophy via the activation of mammalian target of rapamycin complex 1 (mTORC1).

Conclusions A-PDK1KO mice closely mimic the cardiac phenotypes and metabolic alterations observed in human DbCM and exhibit impaired BCAA metabolism in the heart. This model may contribute to a better understanding of DbCM pathophysiology and to the development of novel therapies for this disease.

Keywords Diabetic cardiomyopathy, Branched-chain amino acid, Heart failure, Diabetes mellitus, Cardiac metabolism

*Correspondence:
Manabu Nagao
mnagao@med.kobe-u.ac.jp

Full list of author information is available at the end of the article



© The Author(s) 2025. **Open Access** This article is licensed under a Creative Commons Attribution-NonCommercial-NoDerivatives 4.0 International License, which permits any non-commercial use, sharing, distribution and reproduction in any medium or format, as long as you give appropriate credit to the original author(s) and the source, provide a link to the Creative Commons licence, and indicate if you modified the licensed material. You do not have permission under this licence to share adapted material derived from this article or parts of it. The images or other third party material in this article are included in the article's Creative Commons licence, unless indicated otherwise in a credit line to the material. If material is not included in the article's Creative Commons licence and your intended use is not permitted by statutory regulation or exceeds the permitted use, you will need to obtain permission directly from the copyright holder. To view a copy of this licence, visit <http://creativecommons.org/licenses/by-nc-nd/4.0/>.

Background

Type 2 diabetes mellitus (T2DM) is a metabolic disease characterized by persistent hyperglycemia and systemic insulin resistance [1]. There are more than 500 million individuals with diabetes mellitus (DM) worldwide, and its prevalence is expected to increase, particularly that of T2DM [2, 3]. Individuals with T2DM are highly susceptible to cardiovascular disease, which is a major cause of death and disability [4]. Notably, T2DM is an independent risk factor for developing heart failure (HF), and HF patients with DM have a worse prognosis and quality of life [5, 6]. Especially, while a healthy heart maintains metabolic flexibility by efficiently utilizing various energy substrates, including fatty acids and carbohydrates, a failing heart undergoes a significant shift in substrate dependence, with its utilization patterns changing drastically depending on the pathophysiology, stage, and severity of HF [7, 8]. The pathophysiological association between HF and DM has been documented over the past few decades. A specific type of cardiomyopathy termed diabetic cardiomyopathy (DbCM) was first described in diabetic patients in 1972 by Rubler et al. [9]. DbCM is characterized by clinical HF despite the absence of coronary artery disease, hypertension, and valvular heart disease [1]. DbCM represents one of the major public health problems, but its mechanisms and effective therapies remain to be elucidated [10]. Although analyses of various animal models of T2DM have led to active studies exploring the molecular mechanisms that contribute to a better understanding of the pathogenesis of DbCM [11, 12], each model has inherent limitations or disadvantages, such as pharmacological or long-term dietary interventions [13].

Previously, we generated adipocyte-specific 3'-phosphoinositide-dependent kinase 1 (PDK1)-deficient (A-PDK1KO) mice [14, 15]. PDK1 is a key kinase involved in the insulin signaling pathway; it activates downstream kinases, including Akt and ribosomal protein S6 kinase, by phosphorylation [16]. We previously proposed that insulin signaling in adipocytes plays critical roles in the regulation of leukotriene B4 (LTB4) production via the PDK1-FOXO1 pathway. The genetic deletion of PDK1 in adipocytes led to the development of hyperglycemia, an increase in body weight, and systemic insulin resistance, including in skeletal muscle and the liver, in mice fed a normal diet [14]. However, it is unclear whether A-PDK1KO mice exhibit cardiac insulin resistance followed by the development of DbCM-like phenotypes, including cardiac hypertrophy and fibrosis.

Numerous studies have reported that metabolic alterations occur in diabetic hearts and are strongly related to the pathophysiology of DbCM [17–20]. In particular, the relationships between impaired branched-chain amino acid (BCAA) metabolism and HF pathophysiology have

been intensively investigated in recent studies [21–26], whereas relevant findings on the metabolic regulation of BCAA metabolism in diabetic hearts are limited. Herein, using A-PDK1KO mice, we investigated BCAA metabolism in insulin-resistant hearts by using a novel mouse model of DbCM. This model may increase our understanding of the molecular mechanisms of DbCM and related metabolic remodeling, which may also provide new insight into the treatment of DbCM.

Methods

Animal experiments

The details of the A-PDK1KO mice were described previously [14, 15]. To generate A-PDK1KO mice, PDK1 flox/flox mice [27] were crossed with Adipoq-Cre mice [28]. PDK1flox/flox mice were used as controls. The mice were sacrificed in a randomly fed state at the age of 10–11 weeks unless indicated otherwise. Tissues were collected, snap frozen in liquid nitrogen and subsequently stored at -80°C until further analysis.

BT2 treatment

BT2, a branched chain ketoacid dehydrogenase kinase (BCKDK) inhibitor (3,6-dichlorobenzo(b)thiophene-2-carboxylic acid, BT2; Santacruz, #sc-276559B), was administered orally to A-PDK1KO mice at 4 to 5 weeks of age after weaning for a duration of 4 weeks. Based on a previous study [29], BT2 was dissolved in a 10 mg/mL solution containing 5% DMSO, 10% Kolliphor EL (Sigma, #C5135), and 85% of 0.1 M Na-bicarbonate, pH 9.0 (Bio BASIC INC, #AS88-60066), and administered at a dose of 40 mg/kg/day. Mice were fasted for 5 h prior to tissue collection.

Metabolite quantification with liquid chromatography–mass spectrometry (LC–MS/MS)

Amino acids and branched-chain α -keto acids (BCKAs) were measured by LC–MS/MS as previously described [30, 31]. A mixture of 10 μL of plasma, 10 μL of an internal standard mixture of amino acids (FujiFilm-Wako, #293-73701), 10 μL of KIV- $^{13}\text{C}_5$ (Cambridge Isotope Laboratories, #CLM-4418-PK) and 470 μL of cold methanol (total volume of 500 μL) was vortexed and incubated on ice for 1 h. The mixture was centrifuged at 15,000 rpm for 10 min. After filtration through 0.22- μm pore centrifugal filters (Millipore, # UFC30GV0S), the supernatant was subjected to LC–MS/MS. The system consisted of a QTRAP 6500 (Sciex) instrument equipped with a Shimadzu LC-30AD HPLC system. For amino acid analysis, an Intrada Amino Acid column (100 mm \times 3.0 mm, 3.0 μm , Imtakt Co.) was used with an acetonitrile/formic acid/100 mM ammonium formate gradient of 100:0.1:0 to 0:0:100 (v/v/v) at a flow rate of 0.6 mL/min. For BCKA analysis, an Intrada Organic Acid column (150 mm \times

3.2 mm, 3.0 μ m, Imtakt Co.) was used with an acetonitrile/water/formic acid/100 mM ammonium formate gradient of 10:90:0.1:0 to 10:0:0:90 (v/v/v/v) at a flow rate of 0.2 mL/min. To measure amino acid and BCKA levels, the multiple reaction monitoring (MRM) method was used with the signature ion pairs Q1 (parent ion)/Q3 (characteristic fragment ion) for each molecule. For the measurement of tissue containing amino acids, 10 mg of tissue, 10 μ L of an internal standard mixture of amino acids (FujiFilm-Wako, #293-73701), and 490 μ L of cold methanol were mixed and homogenized by shaking with zirconia beads (AS ONE, #1-5987-05) at 1500 rpm for 15 min. The same procedure was used for the plasma samples.

RNA sequencing data analysis

The quality of the raw paired-end sequence reads was assessed with FastQC (version 0.11.7). Low-quality (<20) bases and adapter sequences were trimmed by Trimmomatic software (version 0.38). Clean reads were mapped to the reference genome using the RNA-seq aligner HISAT2 (version 2.1.0). Gene expression levels were quantified by using featureCounts (version 1.6.3) to count reads mapped to each gene. The raw read counts were normalized to fragments per kilobase of transcript per million (FPKM) values. A heatmap of the expression of genes involved in each metabolic pathway was created from the FPKM values and is illustrated as the log₂-fold change. Principal component analysis (PCA) was performed on the normalized counts, and then, each sample was projected onto the 2D plane defined by the first and second PCA axes using the R packages stats (Version 3.6.1) and gplots (Version 3.0.1.1). RNA sequencing data are available from the NCBI Gene Expression Omnibus (GEO) database under accession number GSE268260.

Western blot analysis

Western blot analysis was conducted as previously reported [32]. Antibodies against the following proteins were used: phospho-Akt (Ser473) (Cell Signaling, #4060), Akt (Cell Signaling, #9272), phospho-BCKDE1A (Ser293) (BETHYL, #A304-672 A), BCKDHA (BETHYL, #A303-790 A), BCKDK (Sigma-Aldrich, #HPA017995), p70-S6K (Cell Signaling, #49D7), phospho-p70-S6K (Cell Signaling, #9234), and GAPDH (Sigma-Aldrich, #G8795).

Quantitative real-time polymerase chain reaction (qPCR)

Total RNA was isolated with a RNeasy Mini kit (Qiagen, #74106), and cDNA was synthesized by using a ReverTra Ace qPCR RT Master Mix kit (TOYOBO, #FSQ-201) following the manufacturer's protocol. qPCR analysis was performed as previously described [30] using TaqMan Primer-Probe Mix. Gene transcript levels were measured with a Thermal Cycler Dice Real Time System

II (Takara). Relative expression was normalized to the expression level of GAPDH. The following TaqMan probes used for qPCR were purchased from Thermo Fisher Scientific: mouse Nppa (Mm01255747_g1), mouse Nppb (Mm01255770_g1), mouse Myh7 (Mm00600555_m1), mouse Col1a1 (Mm00801666_g1), mouse Col3a1 (Mm00802300_m1), mouse Postn (Mm01284919_m1), and mouse Gapdh (Mm99999915_g1).

Echocardiography

Transthoracic two-dimensional echocardiography (Affiniti 70, Philips) was performed as previously reported [30]. Mice were anesthetized with low-dose isoflurane during echocardiography. The parasternal short-axis view was scanned to obtain M-mode images to analyze the left ventricular end-diastolic dimension (LVDd), left ventricular end-systolic dimension (LVDs), interventricular septum thickness at diastole (IVSd), and posterior wall thickness at diastole (PWd), followed by the calculation of the relative wall thickness (RWT) [$RWT = (IVSd + PWd)/LVDd$] and percent fractional shortening (%FS).

Body composition analysis

The mice were anesthetized, and a whole-body scan was conducted using an X-ray computed tomography (CT) scanner designed for experimental animals (LaTheta LCT-200, Hitachi Aloka Medical, Tokyo, Japan). The software accompanying the LCT-200 was used to measure fat mass.

Histological staining

For histological analysis, heart tissues were embedded in optimal cutting temperature compound (Sakura Finetek, #45833). The tissue blocks were sliced into 10- μ m thick sections, and cardiac hypertrophy and lipid accumulation were assessed with hematoxylin and eosin (HE), Masson's trichrome staining, and Oil Red O staining, respectively [30, 33]. Microscopy images of the sections were captured using an OLYMPUS DP70 camera (OLYMPUS, Japan). The myocyte cross-sectional area and Oil Red O staining area were quantified by using ImageJ software.

Measurement of blood glucose and free fatty acids

The plasma glucose and free fatty acid levels were measured with a LabAssay Glucose kit (FujiFilm-Wako, #298-65701) and a LabAssay NEFA kit (FujiFilm-Wako, #294-63601) according to the manufacturers' protocols.

Measurement of triglycerides in cardiac tissue

The triglyceride (TG) levels in the cardiac tissue of mice were measured using the Adipogenesis Assay Kit (Sigma, #MAK040) according to the manufacturer's protocol. The obtained values were normalized to tissue weight.

Malondialdehyde assay

Malondialdehyde (MDA) levels in 10 mg of heart tissue were measured using the MDA Assay Kit (Dojindo, #341-09961) according to the manufacturer's protocol.

Statistical analyses

All the statistical analyses were conducted using GraphPad Prism software version 10.1.0 (GraphPad Software). The normality of the data was assessed using the Shapiro–Wilk test. Differences between two groups were determined using an unpaired Student's *t* test (2-tailed) for parametric variables or the Mann–Whitney test for nonparametric variables. Correlations were evaluated by using Pearson's correlation test. All the data are expressed as means \pm standard errors (SEs). The threshold for significance was $P < 0.05$.

Results

A-PDK1KO mice developed cardiac insulin resistance

A-PDK1KO mice exhibited an increasing trend in blood glucose levels, body weight, and lean mass compared to control mice, while fat mass was decreased (Fig. 1A–D).

To evaluate cardiac insulin resistance, we examined the cardiac levels of phosphorylated Akt, a key component of the insulin signaling pathway. Phospho-AKT levels were significantly decreased in A-PDK1 KO mice, suggesting the suppression of insulin signal transduction in the heart (Fig. 1E).

A-PDK1KO mice exhibited cardiac hypertrophy

We investigated the cardiac phenotypes of A-PDK1KO mice. Compared with control mice, A-PDK1KO mice had greater heart weights (HWs), heart weight-to-body weight (HW/BW) ratios, and heart weight-to-tibial length (HW/TL) ratios (Fig. 2A). Consistent with the increased heart size of the A-PDK1KO mice (Fig. 2B), histological analysis revealed that the cross-sectional area of the left ventricular myocardium was markedly larger in the PDK1-KO mice than in the control mice (Fig. 2C).

In addition, we assessed the left ventricular wall thickness and cardiac function of the mice by using echocardiography. Compared with control mice, A-PDK1KO mice showed significant increases in IVSd, PWd, and

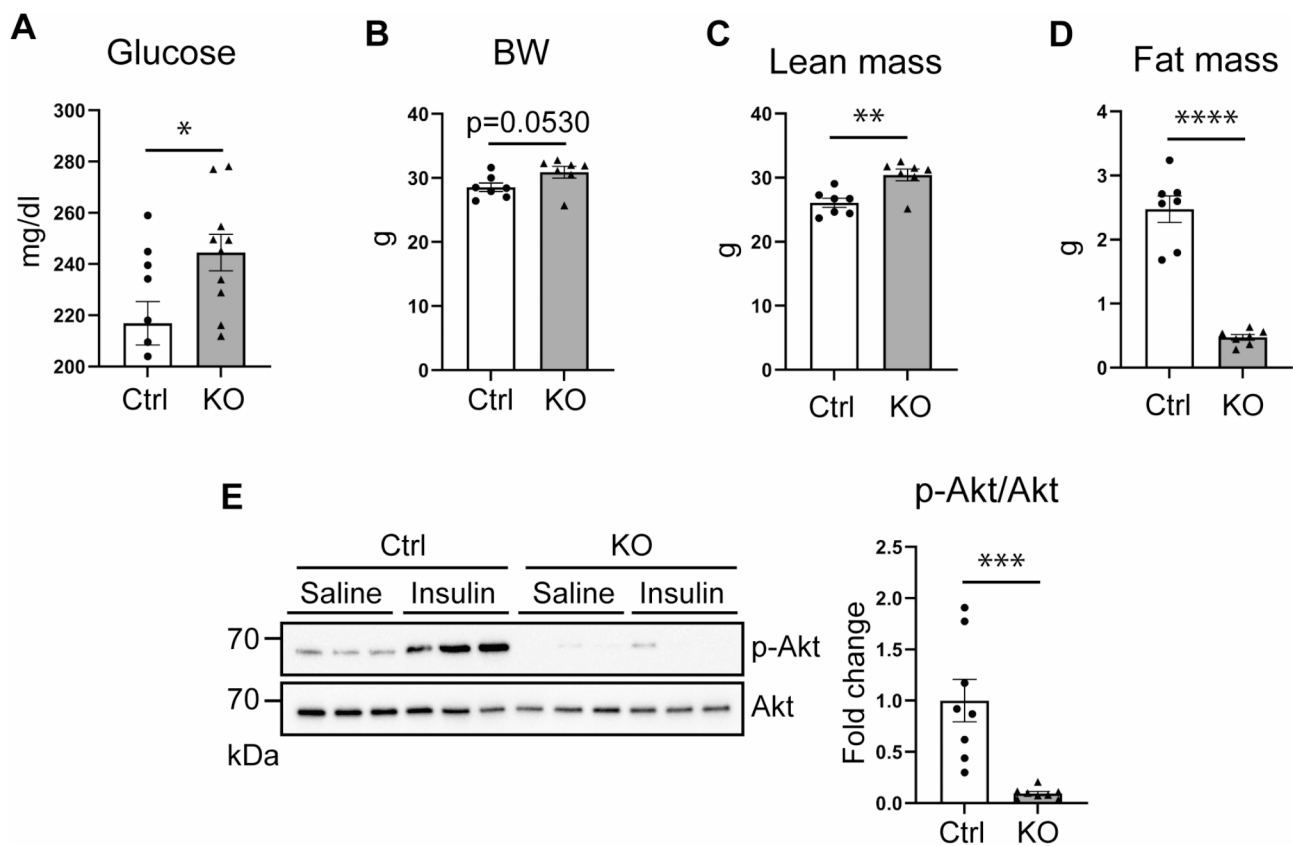


Fig. 1 A-PDK1KO mice exhibited impaired glucose utilization in the heart. **A** Plasma glucose concentrations of control mice and A-PDK1KO mice ($n=10$, each group). **B–D** Body weights **B**, lean mass **C**, and fat mass **D** of 14-week-old mice were measured ($n=7$, each group). **E** Representative images of Western blots of heart tissue and quantification of the band intensity in mice intraperitoneally injected with 0.9% saline or 5 U/kg insulin after a 4-hour fast ($n=8$, each group). The data are shown as means \pm SEs. Significance was calculated by the unpaired Student's *t* test. **p* value < 0.05 , ***p* value < 0.01 , ****p* value < 0.001 , and *****p* value < 0.0001 . BW, body weight; Ctrl, control mice; KO, A-PDK1KO mice

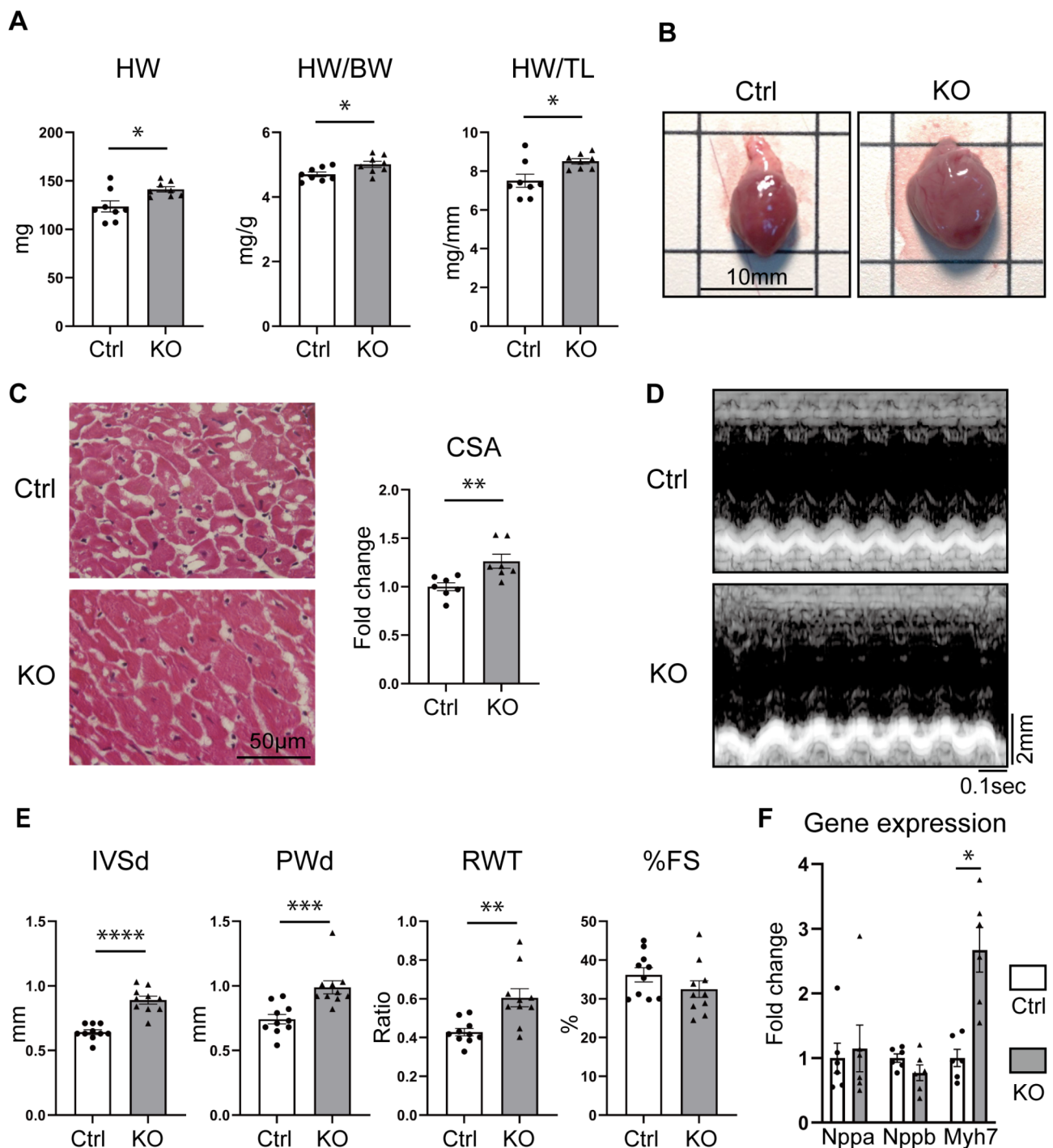


Fig. 2 A-PDK1KO mice exhibited cardiac hypertrophy. **A** Mouse heart weight (HW), heart weight-to-body weight ratio (HW/BW), and heart weight-to-tibia length ratio (HW/TL) ($n=8$, each group). **B** Representative images of the whole heart. Scale bar: 10 mm. **C** Representative images of HE-stained heart sections (scale bar: 50 μ m) and the cross-sectional area (CSA) of the myocardium quantified by ImageJ software and normalized to the average of the control group ($n=7$ per group). **D** Representative images of M-mode echocardiography. **E** Interventricular septum thickness at diastole (IVSd), posterior wall thickness at diastole (PWD), relative wall thickness (RWT), and fractional shortening (%FS) were determined by echocardiography ($n=10$ in each group). **F** Gene expression of Nppa, Nppb, and Myh7 quantified by qPCR and normalized to that of GAPDH ($n=6$ per group). The data are shown as means \pm SEs. Significance was calculated by the unpaired Student's t test. * p value < 0.05 , ** p value < 0.01 , *** p value < 0.001 , **** p value < 0.0001

RWT, while the %FS did not differ significantly between the two groups (Fig. 2D, E).

Furthermore, we assessed the gene expression of cardiac hypertrophy markers. Myosin heavy chain 7 (Myh7) expression was increased in the A-PDK1KO mice, whereas there was no significant difference in the expression levels of natriuretic peptide A (Nppa) and natriuretic peptide B (Nppb) between the two groups (Fig. 2F). Evaluation of cardiac fibrosis revealed a significant increase in Collagen 1a1 (Col1a1) expression in A-PDK1KO mice (Figure S1A). However, Masson's trichrome staining showed no significant difference in fibrotic areas compared to control mice, suggesting a pro-fibrotic state (Figure S1B).

Expression of metabolic pathway genes in the hearts of A-PDK1KO mice

RNA sequencing was conducted to analyze the transcriptional differences between the hearts of control and A-PDK1KO mice. Principal component analysis (PCA) revealed a clear separation between the two groups. The two components of the PCA (PC1 and PC2) indicated that the gene expression patterns of the cardiac tissues of the A-PDK1KO mice were different from those of the control mice (Fig. 3A). A heatmap was generated to depict the transcript levels of the genes relevant to BCAA, fatty acid, and glucose metabolism (Fig. 3B). The expression of genes involved in fatty acid metabolism, such as *Acadm*, *Decr1*, *Ech1*, *Acaa2*, and *Slc25A20*,

was significantly increased in the hearts of A-PDK1KO mice. Intriguingly, the expression of BCAA transporters, including solute carrier family 7 member 5 (*SLC7a5*), was significantly upregulated in A-PDK1KO mice, suggesting increased uptake of BCAAs in the diabetic heart; however, there was no significant difference in the expression of BCAA catabolic genes, such as branched-chain aminotransferase (*BCAT*), *BCKDK*, and the protein phosphatase Mg (2+)/Mn (2+)-dependent 1 K (*Ppm1k*) (Fig. 3B).

Cardiac BCAA metabolism is impaired in A-PDK1KO mice

To better understand BCAA metabolism in A-PDK1KO mice, we measured blood amino acid levels by LC-MS/MS (Fig. 4A). The levels of all three BCAAs were greater in A-PDK1KO mice than in control mice (Fig. 4B). Consistent with the increase, the levels of α -keto-isocaproate (KIC) and α -keto- β -methylvalerate (KMV), BCKAs of leucine and isoleucine, respectively, were significantly increased in the KO mice (Fig. 4C). Next, we assessed cardiac amino acid levels in these model mice (Fig. 5A). Leucine and isoleucine levels were significantly increased in the A-PDK1KO mice (Fig. 5B). Additionally, all BCAAs were significantly elevated in the skeletal muscle of A-PDK1KO mice (Figure S2A). To elucidate the mechanism underlying the increase in blood and heart BCAA levels in A-PDK1KO mice, we assessed the protein expression of key enzymes involved in BCAA oxidation. The BCAA catabolic pathway is shown in Fig. 5C. Phospho-branched-chain α -keto acid dehydrogenase

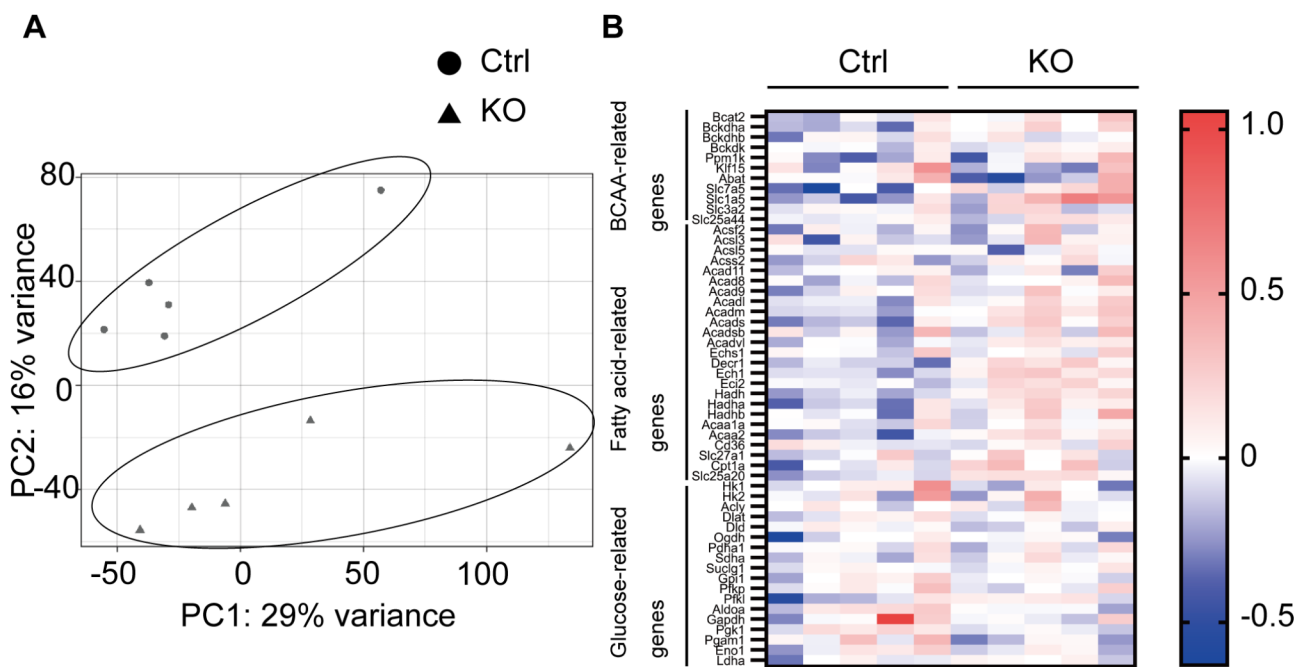


Fig. 3 RNA sequencing of heart tissue. **A** Principal component analysis (PCA) of RNA sequencing data for heart tissue from mice ($n=5$ per group). **B** A heatmap of gene expression related to the indicated metabolic pathways in heart tissue was created from fragments per kilobase of transcript per million (FPKM) values and is illustrated as the log₂-fold change ($n=5$, each group)

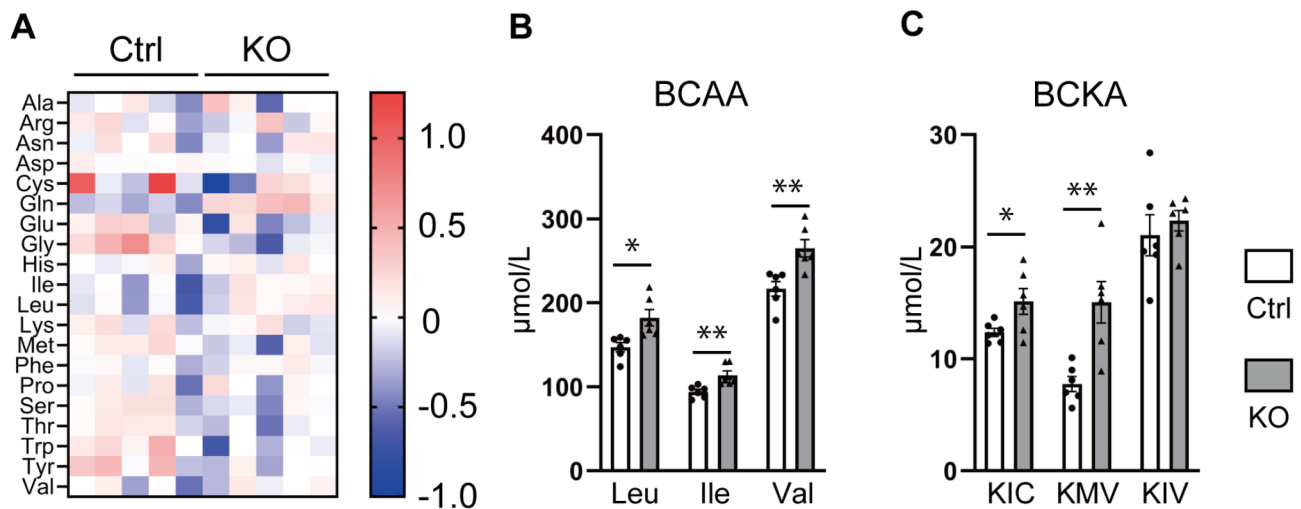


Fig. 4 Blood BCAA levels were increased in A-PDK1KO mice. **A** Heatmap of amino acid concentrations in mouse blood, shown as log₂-fold changes. The values are normalized to the median of each amino acid concentration ($n=5$, each group). **B** Blood concentrations of BCAAs (leucine (Leu), isoleucine (Ile), and valine (Val)) and BCKAs (α -keto-isocaproate (KIC), α -keto- β -methylvalerate (KMV), and α -keto-isovalerate (KIV)) were determined by LC-MS ($n=6$ per group). The data are shown as means \pm SEs. Significance was calculated by the unpaired Student's *t* test or the Mann-Whitney *U* test, as appropriate. **p* value < 0.05, and ***p* value < 0.01

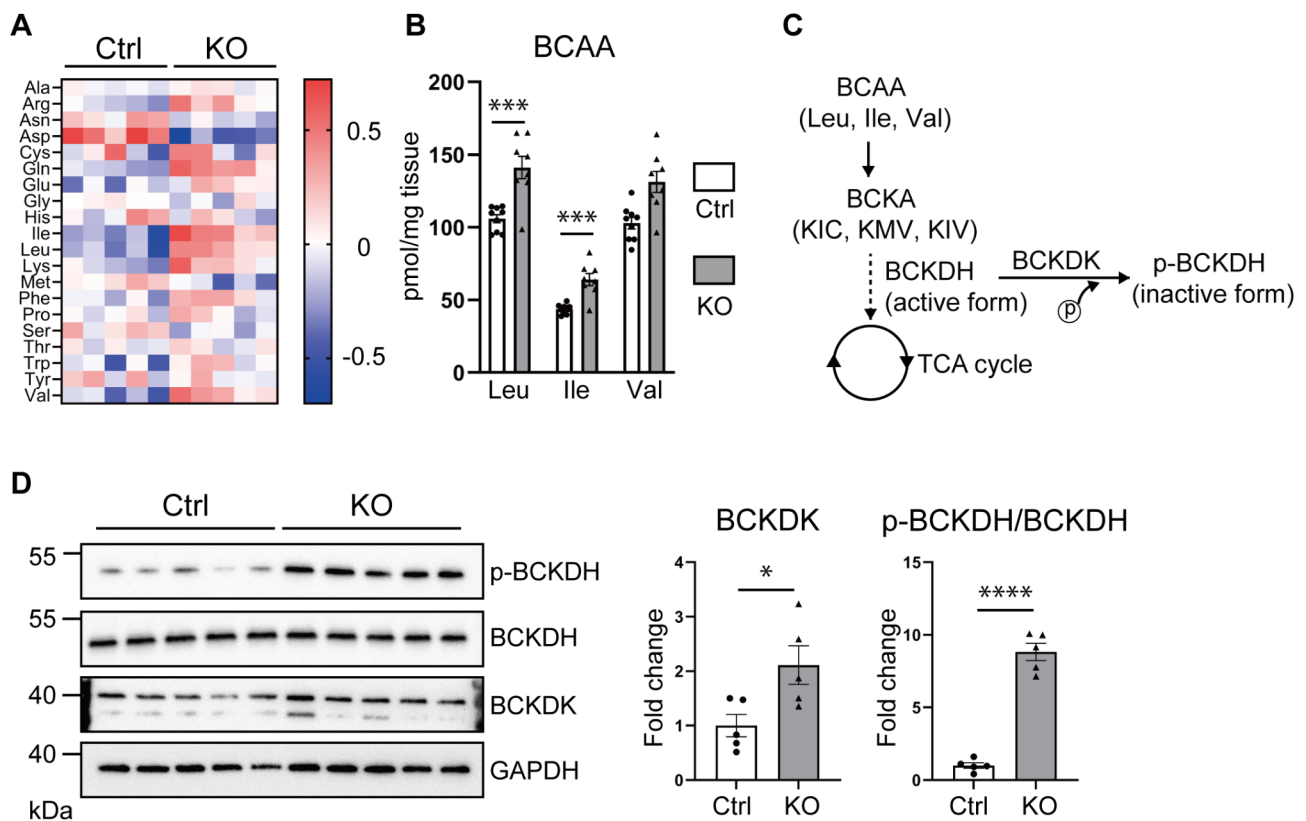


Fig. 5 Cardiac BCAA metabolism was impaired in A-PDK1KO mice. **A** Heatmap of amino acid content in mouse heart tissue, shown as the log₂-fold change. The values are normalized to the median content of each amino acid ($n=5$, each group). **B** BCAA levels in mouse heart tissue were analyzed by LC-MS ($n=8-9$ per group). **C** Schematic diagram of the BCAA oxidation pathway. **D** Western blot analysis of BCKDK and phospho-BCKDH in the heart tissue of mice; the expression levels of BCKDK and phospho-BCKDH were normalized to those for GAPDH and BCKDH, respectively. ($n=5$, each group). The data are shown as means \pm SEs. Significance was calculated by the unpaired Student's *t* test. **p* value < 0.05, ****p* value < 0.001, and *****p* value < 0.0001. Leu, leucine; Ile, isoleucine; Val, valine; KIC, α -keto-isocaproate; KMV, α -keto- β -methylvalerate; and KIV, α -keto-isovalerate

(BCKDH) and BCKDK expression was clearly greater in the KO mice than in the control mice, suggesting that cardiac BCAA oxidation was suppressed in the A-PDK1KO mice (Fig. 5D). Furthermore, we evaluated fatty acid (FA) catabolism in the mice and found that plasma free fatty acid (FFA) levels were increased in the A-PDK1KO mice (Figure S3A). In this context, cardiac lipid accumulation, as estimated by triglyceride (TG) content and Oil Red O staining, tended to increase in the A-PDK1KO mice (Figure S3B–D). Moreover, MDA, a marker of oxidative stress, was significantly elevated in the hearts of the KO group (Figure S4A).

Activation of mTORC1 signaling was associated with cardiac hypertrophy in A-PDK1KO mice

To reveal the mechanisms that cause cardiac hypertrophy in diabetic cardiomyopathy, we focused on mammalian target of rapamycin complex 1 (mTORC1) signaling. Leucine is known to be a key signaling molecule that activates the mTORC1 pathway [34]. The blood leucine concentration was positively correlated with heart weight normalized to body weight (Fig. 6A). We assessed the phosphorylation of p70-S6 kinase (S6K), a downstream substrate of mTORC1. Phospho-S6K was significantly increased in the hearts of the A-PDK1KO mice (Fig. 6B).

To test the hypothesis that leucine accumulation in the heart due to impaired BCAA metabolism activates the mTOR signaling pathway and induces cardiac hypertrophy in A-PDK1KO mice, we administered BT2 to the KO mice for 4 weeks after weaning (Fig. 7A). Interestingly, BT2 treatment suppressed body weight gain, reduced heart weight in mice, and improved left ventricular wall thickening, as assessed by echocardiography (Figure S5A, Fig. 7B–D). Measurement of BCAAs in cardiac tissue and plasma showed a significant reduction in all BCAAs in the BT2-treated group (Fig. 7E). Consistent with

these findings, BT2 suppressed the phosphorylation of BCKDH and S6K in cardiac tissue (Fig. 7F, G), suggesting that the leucine-mTORC1 axis is associated with cardiac hypertrophy in this mouse model.

Discussion

Previously, we demonstrated that A-PDK1KO mice exhibit adipose tissue dysfunction due to impaired insulin signaling in adipose tissue. This dysfunction leads to systemic metabolic abnormalities, including insulin resistance in skeletal muscle, hyperinsulinemia, hyperglycemia, elevated circulating FFAs, and reduced adiponectin levels [14]. In the present study, we investigated the cardiac phenotype of A-PDK1KO mice and found that these mice exhibit prominent cardiac insulin resistance and cardiac hypertrophy, both of which are characteristic features of DbCM [9, 35, 36]. Elevated circulating FFA levels may have increased fatty acid influx into the heart, potentially leading to lipid accumulation and subsequent lipotoxicity, while also promoting excessive fatty acid oxidation that may have enhanced the production of reactive oxygen species (ROS). These components are considered to contribute to cardiac insulin resistance and myocardial injury, ultimately resulting in the development of the DbCM phenotype. Moreover, we investigated a novel mechanism in this study and proposed a potential link between BCAA metabolic disturbance and the pathogenesis of DbCM. We observed the downregulated expression of the key enzymes involved in BCAA catabolism and subsequent BCAA accumulation in the hearts of A-PDK1KO mice, indicating that BCAA oxidation is impaired in DbCM as well as HF. Furthermore, the improvement in BCAA catabolism induced by drug treatment reduced leucine content in the heart, leading to the attenuation of cardiac hypertrophy, presumably

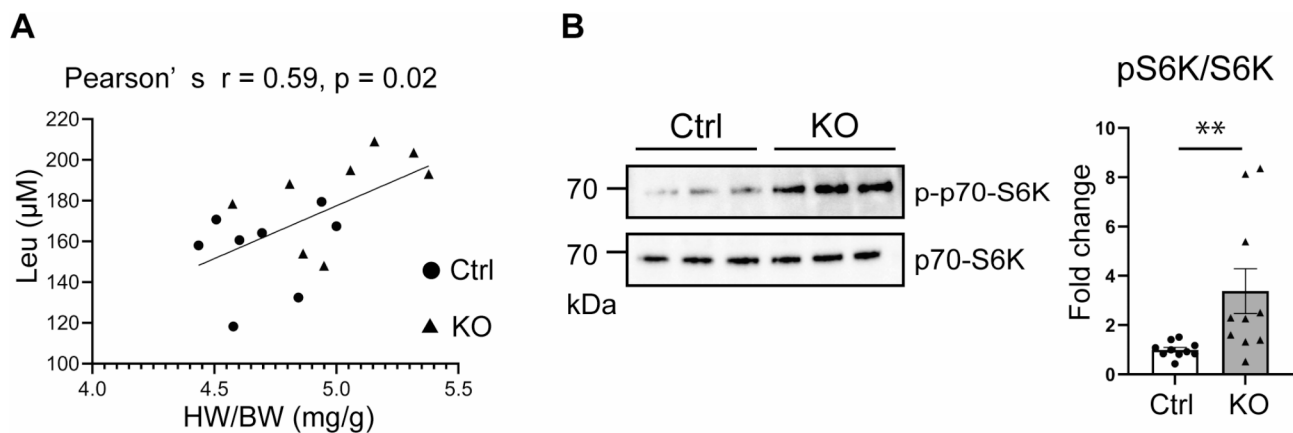


Fig. 6 Association between leucine-mTOR signaling and cardiac hypertrophy in A-PDK1KO mice. **A** Correlation between blood leucine levels and the heart weight-to-body weight ratio (HW/BW) in mice (Ctrl; $n=8$, KO; $n=8$). **B** Western blot analysis of phospho-S6K (p-p70-S6K) and S6K (p70-S6K) in the heart tissue of mice ($n=10$, each group). The data are shown as means \pm SEs. Significance was calculated by the unpaired Student's *t* test. **p* value < 0.05

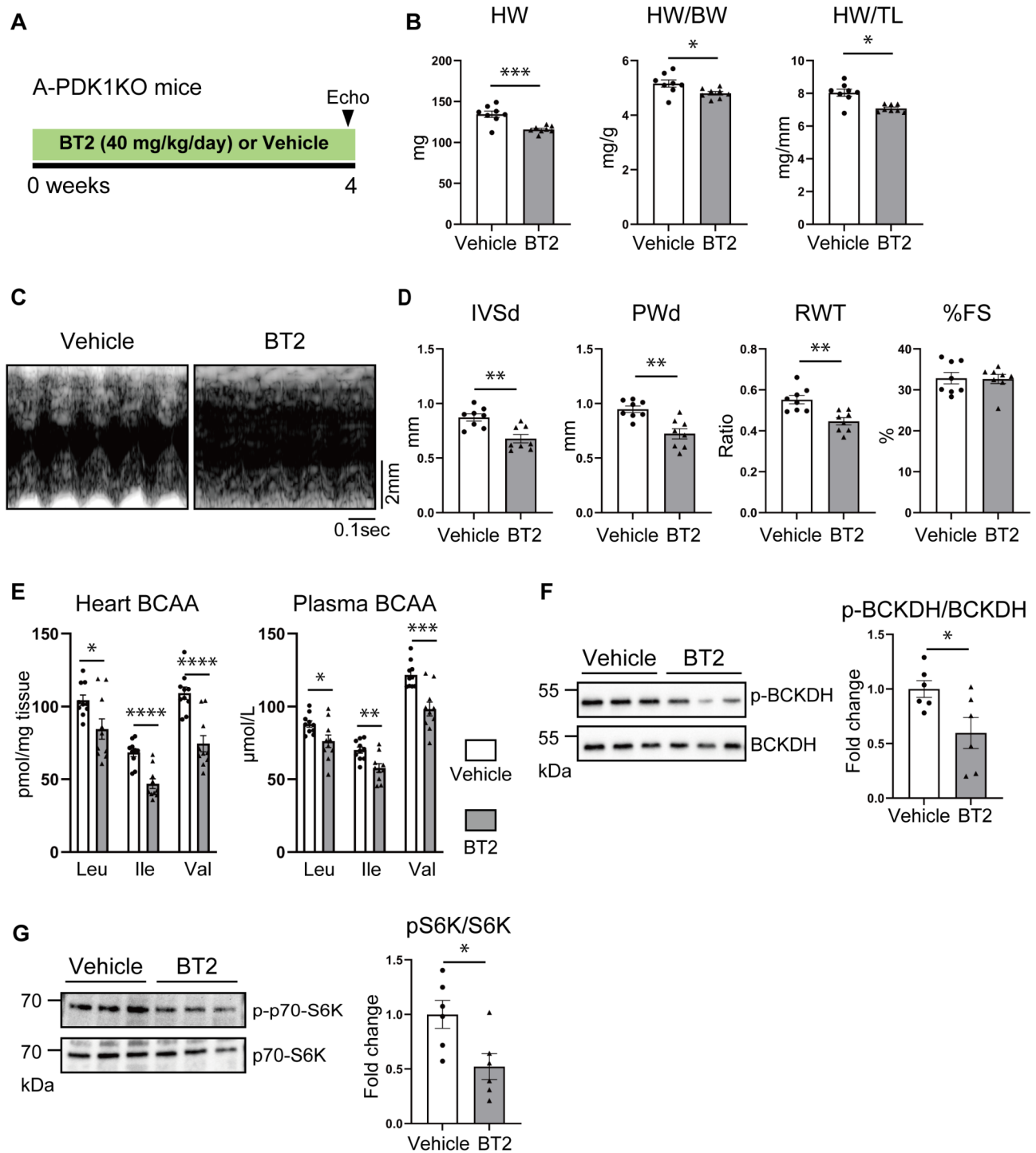


Fig. 7 BT2 treatment mitigated cardiac hypertrophy in A-PDK1KO mice. **A** Scheme of the experimental approach. 4–5-week-old A-PDK1KO mice were orally administered 40 mg/kg/day of BT2 or vehicle for 4 weeks. **B** Mouse heart weight (HW), heart weight-to-body weight ratio (HW/BW), and heart weight-to-tibia length ratio (HW/TL) ($n=8$, each group). **C** Representative images of M-mode echocardiography. **D** Interventricular septum thickness at diastole (IVSd), posterior wall thickness at diastole (PWd), relative wall thickness (RWT), and fractional shortening (%FS) were measured by echocardiography ($n=8$, each group). **E** BCAA content in the cardiac tissue or plasma of A-PDK1KO mice treated with BT2 or vehicle ($n=10$, each group). **F** Western blot analysis of BCKDH and phospho-BCKDH in the heart tissue of the mice; the expression levels of phospho-BCKDH were normalized to those for BCKDH. ($n=6$, each group). **G** Western blot analysis of phospho-S6K (p-p70-S6K) and S6K (p70-S6K) in the heart tissue of mice ($n=6$, each group). The data are shown as means \pm SEs. Significance was calculated by the unpaired Student's t test or the Mann-Whitney U test, as appropriate. *p value < 0.05, **p value < 0.01, ***p value < 0.001, and ****p value < 0.0001

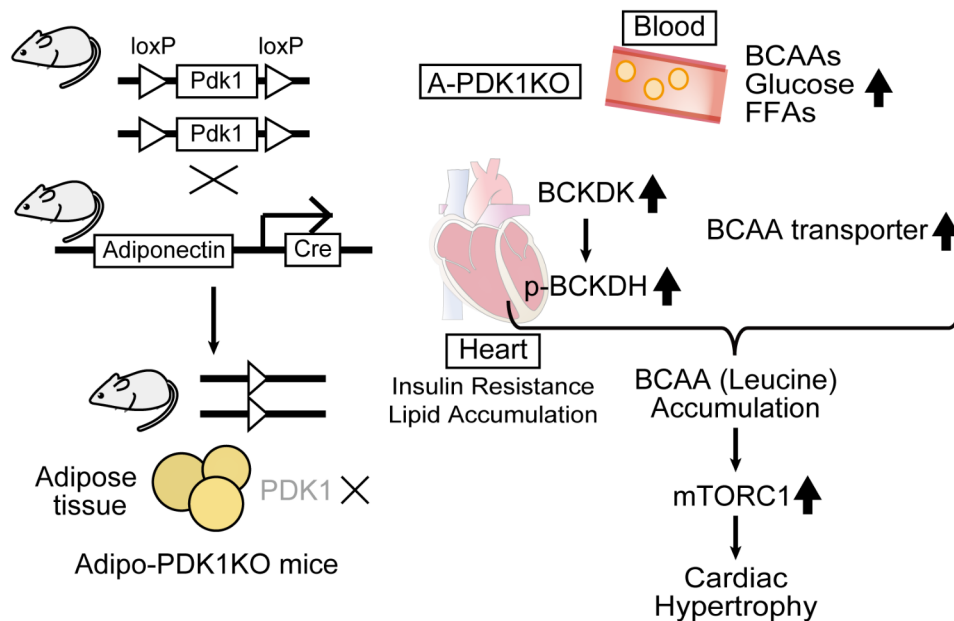


Fig. 8 A schematic model of the underlying mechanism of cardiac hypertrophy in A-PDK1KO mice as a model of diabetic cardiomyopathy. BCAA, branched-chain amino acid; FFAs, free fatty acids; BCKDK, branched chain ketoacid dehydrogenase kinase; and mTORC1, mammalian target of rapamycin complex 1

through the suppression of the mTOR signaling pathway (Fig. 8).

The relationship between BCAA oxidation and insulin resistance was first reported in 1969, and plasma BCAA levels were shown to be increased in obese individuals. Since then, various studies have confirmed that elevated blood BCAA levels are associated with insulin resistance in humans and several rodent models of obesity or T2DM [37–41]. This increase in BCAAs is thought to be partly due to the activation of tissue proteolysis induced by insufficient insulin levels [42, 43]. Regarding cardiac BCAA metabolism, cardiac BCAA oxidation is impaired in the heart of patients with cardiovascular diseases and in the heart of rodent models of insulin resistance [20, 25, 26, 44, 45]. The suppression of BCAA catabolic enzymes, followed by the increased accumulation of BCAAs, occurs in the heart tissue of patients with dilated cardiomyopathy or HF with preserved ejection fraction (HFpEF) [25, 26]. Although RNA sequencing indicated no significant difference in the expression of BCAA metabolic enzyme genes, A-PDK1KO mice exhibited increased BCKDK protein levels and enhanced BCKDH phosphorylation as a post-translational modification in the heart. In general, gene expression levels do not necessarily correlate with protein expression or post-translational modifications. In this study, we consider that the observed impairment in BCAA metabolism is caused by the upregulation of BCKDK and the consequent phosphorylation of BCKDH. Importantly, BCKDK has been investigated as a therapeutic target for HF. The BCKDK inhibitor BT2 has been shown to improve cardiac

function and attenuate detrimental remodeling in murine models of pressure overload-induced HF by enhancing BCAA oxidation [21, 22]. Interestingly, Murashige et al. demonstrated that, contrary to previous findings, the enhancement of whole-body BCAA oxidation, including that in skeletal muscle, contributes to cardiac protection. However, in their model mice with cardiac-specific enhancement of BCAA oxidation, no cardioprotective effects were observed [46]. Since their mouse model is not a DbCM model, it is meaningful to use A-PDK1KO mice to study the regulation of BCAA metabolism in DbCM.

BCAAs are known to function as signaling molecules. Leucine promotes protein synthesis by regulating protein translation, ribosome biogenesis, and autophagy through the mTORC1 pathway [34, 47–50]. Neishabouri et al. reported that mTORC1 activation induced by BCAA accumulation is responsible for cardiac hypertrophy. Similarly, our data showed that plasma levels of BCAAs, particularly that of leucine, were correlated with cardiac hypertrophy and that mTORC1 pathway activation occurred in the hearts of A-PDK1KO mice. In our experiment administering BT2 to A-PDK1KO mice, a reduction in leucine content within cardiac tissue was observed, accompanied by the suppression of mTOR signaling and a subsequent attenuation of cardiac hypertrophy. Furthermore, we found that the expression of genes involved in BCAA transport was elevated in the hearts of A-PDK1KO mice, suggesting that BCAA uptake from the blood stream into cardiomyocytes is increased in DbCM. Regarding the uptake and release of amino acids in HF,

a previous study assessed arteriovenous gradients of circulating metabolites by simultaneously collecting blood from the radial artery and coronary sinus of patients with atrial fibrillation and demonstrated that the uptake of all three BCAAs (Val, Leu, and Ile) from the circulation into the heart is greater than the uptake of other amino acids [51]. These findings suggest that the BCAA-mTOR axis and BCAA transporters could be new therapeutic targets for HF treatment and that A-PDK1KO mice can be utilized to evaluate the impact of new drugs related to the BCAA metabolic pathway on cardiac phenotypes induced by DbCM.

Over the past few decades, various T2DM or obesity models induced by dietary manipulation, pharmacological intervention, or genetic modification have been used as DbCM models. Among them, *ob/ob* mice and *db/db* mice, which are congenitally deficient in either leptin or leptin receptor, respectively, have been frequently employed as genetic models of insulin resistance and T2DM [52, 53]. Consistent with these genetic models, A-PDK1KO mice manifested hyperglycemia, hyperinsulinemia, and increased blood FFAs without being fed a special diet, such as a high-fat diet [14]. Notably, A-PDK1KO mice naturally developed cardiac hypertrophy in the absence of genetic modifications in the heart, which seems to more closely mimic the pathophysiology of DbCM. However, cardiac BCAA metabolism in *ob/ob* and *db/db* mice has not been fully elucidated. A study using *db/db* mice fed a high-fat diet did not show a significant change in cardiac BCAA levels or BCAA-related enzyme expression between control mice and *db/db* mice [54]. In A-PDK1KO mice, impaired cardiac BCAA catabolism may reflect the same metabolic alterations as those in other organs in patients with T2DM [55]. Further studies are needed to clarify the relationship between the metabolic reprogramming of cardiac BCAA and the pathophysiology of DbCM.

We need to acknowledge that our study has several limitations. First, all experiments were conducted with male mice. Notably, a diurnal rhythm, which is controlled by estrogen and BCKDK activity, occurs in BCAA oxidation in female murine models [56]. Second, we could not estimate the cardiac diastolic function of the A-PDK1KO mice because of performance issues with our ultrasound device. Third, we attempted to measure the cardiac BCKA levels; however, due to high background noise from myocardial tissue, the peaks were detected in LC-MS analysis but did not meet the criteria for reliable quantification and reproducibility. Consequently, we were unable to report the quantitative values. Lastly, since A-PDK1KO mice exhibited a significant increase in BCAA content in skeletal muscle, we cannot exclude the possibility that the elevated BCAA levels in the heart and plasma originate from skeletal muscle.

However, identifying the specific tissue source of BCAAs in vivo remains technically challenging. Therefore, further research is required to address these issues so that the utility of these DbCM model mice can be evaluated appropriately.

Conclusion

A-PDK1KO mice closely mimicked the phenotypes and metabolic alterations in human DbCM and exhibited impaired BCAA catabolism in the heart. This model could contribute to a deeper understanding of the pathology of DbCM and to the development of novel therapies for this disease.

Abbreviations

T2DM	Type 2 diabetes mellitus
DbCM	Diabetic cardiomyopathy
A-PDK1KO	Adipocyte-specific 3'-phosphoinositide-dependent kinase 1-knockout
BCAA	Branched-chain amino acid
BCKA	Branched-chain α -keto acids
mTORC1	Mammalian target of rapamycin complex 1
HF	Heart failure

Supplementary Information

The online version contains supplementary material available at <https://doi.org/10.1186/s12933-025-02725-5>.

Supplementary Material 1.

Acknowledgements

We thank Emiko Yoshida for expert technical assistance.

Author contributions

Junko Asakura: Conceptualization, Animal experiments, Investigation, Writing original Draft. Manabu Nagao: Writing original Draft, Project administration, Funding acquisition. Masakazu Shinohara: Formal analysis. Tetsuya Hosooka: Animal experiments. Naoya Kuwahara: Animal experiments. Makoto Nishimori: Statistical analysis. Hidekazu Tanaka: Resources. Seimi Satomi-Kobayashi: Animal experiments. Sho Matsui: Animal experiments. Tsutomu Sasaki: Data Collection, Animal experiments. Tadahiro Kitamura: Resources. Hiromasa Otake: Supervision. Tatsuhiro Ishida: Supervision. Wataru Ogawa: Conceptualization. Ken-ichi Hirata: Project administration. Ryuji Toh: Supervision.

Funding

This work was supported by the Hyogo Science and Technology Association, SENSHIN Medical Research Foundation, Uehara Memorial Foundation, Japan Diabetes Foundation, Novo Nordisk Pharma Ltd., MSD Life Science Foundation, Mochida Memorial Foundation, Grant-in-Aid for Scientific Research (C) (22K08205), and Grant-in-Aid for Young Scientists (20K17081) from the Ministry of Education, Culture, Sports, Science and Technology of Japan.

Data availability

RNA sequencing data are available from the NCBI Gene Expression Omnibus (GEO) database under accession number GSE268260.

Declarations

Ethics approval and consent to participate

All animal studies were conducted in accordance with institutional guidelines and the Guide for the Care and Use of Laboratory Animals after receiving the approval of Kobe University.

Consent for publication

Not applicable.

Competing interests

The Division of Evidence-based Laboratory Medicine, Kobe University Graduate School of Medicine, was established by an endowment fund from Sysmex Corporation, Japan.

Author details

¹Division of Cardiovascular Medicine, Kobe University Graduate School of Medicine, 7-5-2 Kusunoki-cho, Chuo-ku, Kobe 650-0017, Japan

²Division of Evidence-Based Laboratory Medicine, Kobe University Graduate School of Medicine, 7-5-1 Kusunoki-cho, Chuo-ku, Kobe 650-0017, Japan

³Division of Molecular Epidemiology, Kobe University Graduate School of Medicine, 7-5-1 Kusunoki-cho, Chuo-ku, Kobe, Japan

⁴The Integrated Center for Mass Spectrometry, Kobe University Graduate School of Medicine, 7-5-1 Kusunoki-cho, Chuo-ku, Kobe, Japan

⁵Laboratory of Nutritional Physiology, Graduate School of Integrated Pharmaceutical and Nutritional Sciences, University of Shizuoka, 52-1 Yada, Suruga-ku, Shizuoka 422-8526, Japan

⁶Division of Diabetes and Endocrinology, Department of Internal Medicine, Kobe University Graduate School of Medicine, 7-5-1 Kusunoki-cho, Chuo-ku, Kobe, Japan

⁷Laboratory of Nutrition Chemistry, Division of Food Science and Biotechnology Graduate School of Agriculture, Kyoto University, 7-10-2 Tomogaoka, Suma-ku, Kyoto 654-0142, Japan

⁸Metabolic Signal Research Center, Institute for Molecular and Cellular Regulation, Gunma University, Maebashi, Japan

⁹Division of Nursing Practice, Kobe University Graduate School of Health Sciences, Kobe, Japan

Received: 17 July 2024 / Accepted: 5 April 2025

Published online: 16 April 2025

References

- Pan KL, Hsu YC, Chang ST, Chung CM, Lin CL. The role of cardiac fibrosis in diabetic cardiomyopathy: from pathophysiology to clinical diagnostic tools. *Int J Mol Sci* 2023, 24(10).
- Collaborators GBDD. Global, regional, and National burden of diabetes from 1990 to 2021, with projections of prevalence to 2050: a systematic analysis for the global burden of disease study 2021. *Lancet*. 2023;402(10397):203–34.
- Tinajero MG, Malik VS. An update on the epidemiology of type 2 diabetes: a global perspective. *Endocrinol Metab Clin North Am*. 2021;50(3):337–55.
- Kim AH, Jang JE, Han J. Current status on the therapeutic strategies for heart failure and diabetic cardiomyopathy. *Biomed Pharmacother*. 2022;145:112463.
- Nichols GA, Hillier TA, Erbey JR, Brown JB. Congestive heart failure in type 2 diabetes: prevalence, incidence, and risk factors. *Diabetes Care*. 2001;24(9):1614–9.
- Pazin-Filho A, Kottgen A, Bertoni AG, Russell SD, Selvin E, Rosamond WD, Coresh J. HbA 1c as a risk factor for heart failure in persons with diabetes: the atherosclerosis risk in communities (ARIC) study. *Diabetologia*. 2008;51(12):2197–204.
- Neubauer S. The failing heart—an engine out of fuel. *N Engl J Med*. 2007;356(11):1140–51.
- Lopaschuk GD, Karwi QG, Tian R, Wende AR, Abel ED. Cardiac energy metabolism in heart failure. *Circ Res*. 2021;128(10):1487–513.
- Rubler S, Dlugash J, Yuceoglu YZ, Kumral T, Branwood AW, Grishman A. New type of cardiomyopathy associated with diabetic glomerulosclerosis. *Am J Cardiol*. 1972;30(6):595–602.
- Nakamura K, Miyoshi T, Yoshida M, Akagi S, Saito Y, Ejiri K, Matsuo N, Ichikawa K, Iwasaki K, Naito T et al. Pathophysiology and treatment of diabetic cardiomyopathy and heart failure in patients with diabetes mellitus. *Int J Mol Sci* 2022, 23(7).
- Bugger H, Abel ED. Molecular mechanisms of diabetic cardiomyopathy. *Diabetologia*. 2014;57(4):660–71.
- Murtaza G, Virk HUH, Khalid M, Lavie CJ, Ventura H, Mukherjee D, Ramu V, Bhogal S, Kumar G, Shanmugasundaram M, et al. Diabetic cardiomyopathy—a comprehensive updated review. *Prog Cardiovasc Dis*. 2019;62(4):315–26.
- Heather LC, Hafstad AD, Halade GV, Harmancey R, Mellor KM, Mishra PK, Mulvihill EE, Nabben M, Nakamura M, Rider OJ, et al. Guidelines on models of diabetic heart disease. *Am J Physiol Heart Circ Physiol*. 2022;323(1):H176–200.
- Hosooka T, Hosokawa Y, Matsugi K, Shinohara M, Senga Y, Tamori Y, Aoki C, Matsui S, Sasaki T, Kitamura T, et al. The PDK1-FoxO1 signaling in adipocytes controls systemic insulin sensitivity through the 5-lipoxygenase-leukotriene B(4) axis. *Proc Natl Acad Sci USA*. 2020;117(21):11674–84.
- Imamori M, Hosooka T, Imi Y, Hosokawa Y, Yamaguchi K, Itoh Y, Ogawa W. Thrombospondin-1 promotes liver fibrosis by enhancing TGF-beta action in hepatic stellate cells. *Biochem Biophys Res Commun*. 2024;693:149369.
- Pearce LR, Komander D, Alessi DR. The nuts and bolts of AGC protein kinases. *Nat Rev Mol Cell Biol*. 2010;11(1):9–22.
- Rijzewijk LJ, van der Meer RW, Lamb HJ, de Jong HW, Lubberink M, Romijn JA, Bax JJ, de Roos A, Twisk JW, Heine RJ, et al. Altered myocardial substrate metabolism and decreased diastolic function in nonischaemic human diabetic cardiomyopathy: studies with cardiac positron emission tomography and magnetic resonance imaging. *J Am Coll Cardiol*. 2009;54(16):1524–32.
- Petersen KF, Dufour S, Befroy D, Garcia R, Shulman GI. Impaired mitochondrial activity in the insulin-resistant offspring of patients with type 2 diabetes. *N Engl J Med*. 2004;350(7):664–71.
- Mizuno Y, Harada E, Nakagawa H, Morikawa Y, Shono M, Kugimiya F, Yoshimura M, Yasue H. The diabetic heart utilizes ketone bodies as an energy source. *Metabolism*. 2017;77:65–72.
- Fillmore N, Wagg CS, Zhang L, Fukushima A, Lopaschuk GD. Cardiac branched-chain amino acid oxidation is reduced during insulin resistance in the heart. *Am J Physiol Endocrinol Metab*. 2018;315(5):E1046–52.
- Chen M, Gao C, Yu J, Ren S, Wang M, Wynn RM, Chuang DT, Wang Y, Sun H. Therapeutic effect of targeting branched-chain amino acid catabolic flux in pressure-overload induced heart failure. *J Am Heart Assoc*. 2019;8(11):e011625.
- Uddin GM, Zhang L, Shah S, Fukushima A, Wagg CS, Gopal K, Al Batran R, Pherwani S, Ho KL, Boisvenue J, et al. Impaired branched chain amino acid oxidation contributes to cardiac insulin resistance in heart failure. *Cardiovasc Diabetol*. 2019;18(1):86.
- Santos-Gallego CG, Requena-Ibanez JA, San Antonio R, Ishikawa K, Watanabe S, Picatoste B, Flores E, Garcia-Ropero A, Sanz J, Hajjar RJ, et al. Empagliflozin ameliorates adverse left ventricular remodeling in nondiabetic heart failure by enhancing myocardial energetics. *J Am Coll Cardiol*. 2019;73(15):1931–44.
- Du X, Li Y, Wang Y, You H, Hui P, Zheng Y, Du J. Increased branched-chain amino acid levels are associated with long-term adverse cardiovascular events in patients with STEMI and acute heart failure. *Life Sci*. 2018;209:167–72.
- Sun H, Olson KC, Gao C, Prosdocimo DA, Zhou M, Wang Z, Jeyaraj D, Youn JY, Ren S, Liu Y, et al. Catabolic defect of branched-chain amino acids promotes heart failure. *Circulation*. 2016;133(21):2038–49.
- Hahn VS, Petucci C, Kim MS, Bedi KC Jr, Wang H, Mishra S, Koleini N, Yoo EJ, Margulies KB, Arany Z, et al. Myocardial metabolomics of human heart failure with preserved ejection fraction. *Circulation*. 2023;147(15):1147–61.
- Inoue H, Ogawa W, Asakawa A, Okamoto Y, Nishizawa A, Matsumoto M, Teshigawara K, Matsuki Y, Watanabe E, Hiramatsu R, et al. Role of hepatic STAT3 in brain-insulin action on hepatic glucose production. *Cell Metab*. 2006;3(4):267–75.
- Eguchi J, Wang X, Yu S, Kershaw EE, Chiu PC, Dushay J, Estall JL, Klein U, Maratos-Flier E, Rosen ED. Transcriptional control of adipose lipid handling by IRF4. *Cell Metab*. 2011;13(3):249–59.
- Nishi K, Yoshii A, Abell L, Zhou B, Frausto R, Ritterhoff J, McMillen TS, Sweet I, Wang Y, Gao C, et al. Branched-chain Keto acids inhibit mitochondrial pyruvate carrier and suppress gluconeogenesis in hepatocytes. *Cell Rep*. 2023;42(6):112641.
- Yoshikawa S, Nagao M, Toh R, Shinohara M, Iino T, Irino Y, Nishimori M, Tanaka H, Satomi-Kobayashi S, Ishida T, et al. Inhibition of glutaminase 1-mediated Glutaminolysis improves pathological cardiac remodeling. *Am J Physiol Heart Circ Physiol*. 2022;322(5):H749–61.
- Yoshida N, Yamashita T, Osone T, Hosooka T, Shinohara M, Kitahama S, Sasaki K, Sasaki D, Yoneshiro T, Suzuki T, et al. *Bacteroides* spp. Promotes branched-chain amino acid catabolism in brown fat and inhibits obesity. *iScience*. 2021;24(11):103342.
- Nagao M, Toh R, Irino Y, Mori T, Nakajima H, Hara T, Honjo T, Satomi-Kobayashi S, Shinke T, Tanaka H, et al. beta-Hydroxybutyrate elevation as a compensatory response against oxidative stress in cardiomyocytes. *Biochem Biophys Res Commun*. 2016;475(4):322–8.

33. Saito Y, Yamashita T, Yoshida N, Emoto T, Takeda S, Tabata T, Shinohara M, Kishino S, Sugiyama Y, Kitamura N, et al. Structural differences in bacterial lipopolysaccharides determine atherosclerotic plaque progression by regulating the accumulation of neutrophils. *Atherosclerosis*. 2022;358:1–11.
34. Nicklin P, Bergman P, Zhang B, Triantafellow E, Wang H, Nyfeler B, Yang H, Hild M, Kung C, Wilson C, et al. Bidirectional transport of amino acids regulates mTOR and autophagy. *Cell*. 2009;136(3):521–34.
35. Lee M, Gardin JM, Lynch JC, Smith VE, Tracy RP, Savage PJ, Szklo M, Ward BJ. Diabetes mellitus and echocardiographic left ventricular function in free-living elderly men and women: the cardiovascular health study. *Am Heart J*. 1997;133(1):36–43.
36. Devereux RB, Roman MJ, Paranicas M, O'Grady MJ, Lee ET, Welty TK, Fabsitz RR, Robbins D, Rhoades ER, Howard BV. Impact of diabetes on cardiac structure and function: the strong heart study. *Circulation*. 2000;101(19):2271–6.
37. Badoud F, Lam KP, DiBattista A, Perreault M, Zulyniak MA, Cattrysse B, Stephenson S, Britz-McKibbin P, Mutch DM. Serum and adipose tissue amino acid homeostasis in the metabolically healthy obese. *J Proteome Res*. 2014;13(7):3455–66.
38. Newgard CB, An J, Bain JR, Muehlbauer MJ, Stevens RD, Lien LF, Haqq AM, Shah SH, Arlotto M, Slentz CA, et al. A branched-chain amino acid-related metabolic signature that differentiates obese and lean humans and contributes to insulin resistance. *Cell Metab*. 2009;9(4):311–26.
39. Lackey DE, Lynch CJ, Olson KC, Mostaedi R, Ali M, Smith WH, Karpe F, Humphreys S, Bedinger DH, Dunn TN, et al. Regulation of adipose branched-chain amino acid catabolism enzyme expression and cross-adipose amino acid flux in human obesity. *Am J Physiol Endocrinol Metab*. 2013;304(11):E1175–1187.
40. She P, Van Horn C, Reid T, Hutson SM, Cooney RN, Lynch CJ. Obesity-related elevations in plasma leucine are associated with alterations in enzymes involved in branched-chain amino acid metabolism. *Am J Physiol Endocrinol Metab*. 2007;293(6):E1552–1563.
41. Olson KC, Chen G, Xu Y, Hajnal A, Lynch CJ. Alloisoleucine differentiates the branched-chain aminoacidemia of Zucker and dietary obese rats. *Obes Silver Spring*. 2014;22(5):1212–5.
42. She P, Olson KC, Kadota Y, Inukai A, Shimomura Y, Hoppel CL, Adams SH, Kawamata Y, Matsumoto H, Sakai R, et al. Leucine and protein metabolism in obese Zucker rats. *PLoS ONE*. 2013;8(3):e59443.
43. Welle S, Barnard RR, Statt M, Amatruda JM. Increased protein turnover in obese women. *Metabolism*. 1992;41(9):1028–34.
44. Yang Y, Zhao M, He X, Wu Q, Li DL, Zang WJ. Pyridostigmine protects against diabetic cardiomyopathy by regulating vagal activity, gut microbiota, and branched-chain amino acid catabolism in diabetic mice. *Front Pharmacol*. 2021;12:647481.
45. Ogawa T, Kouzu H, Osanami A, Tatekoshi Y, Sato T, Kuno A, Fujita Y, Ino S, Shimizu M, Toda Y, et al. Downregulation of extramitochondrial BCKDH and its uncoupling from AMP deaminase in type 2 diabetic OLETF rat hearts. *Physiol Rep*. 2023;11(4):e15608.
46. Murashige D, Jung JW, Neinast MD, Levin MG, Chu Q, Lambert JP, Garbincius JF, Kim B, Hoshino A, Marti-Pamies I, et al. Extra-cardiac BCAA catabolism lowers blood pressure and protects from heart failure. *Cell Metab*. 2022;34(11):1749–e17641747.
47. Dreyer HC, Drummond MJ, Pennings B, Fujita S, Glynn EL, Chinkes DL, Dhanani S, Volpi E, Rasmussen BB. Leucine-enriched essential amino acid and carbohydrate ingestion following resistance exercise enhances mTOR signaling and protein synthesis in human muscle. *Am J Physiol Endocrinol Metab*. 2008;294(2):E392–400.
48. Anthony JC, Yoshizawa F, Anthony TG, Vary TC, Jefferson LS, Kimball SR. Leucine stimulates translation initiation in skeletal muscle of postabsorptive rats via a rapamycin-sensitive pathway. *J Nutr*. 2000;130(10):2413–9.
49. Bolster DR, Vary TC, Kimball SR, Jefferson LS. Leucine regulates translation initiation in rat skeletal muscle via enhanced eIF4G phosphorylation. *J Nutr*. 2004;134(7):1704–10.
50. Wolfson RL, Chantranupong L, Saxton RA, Shen K, Scaria SM, Cantor JR, Sabatini DM. Sestrin2 is a leucine sensor for the mTORC1 pathway. *Science*. 2016;351(6268):43–8.
51. Murashige D, Jang C, Neinast M, Edwards JJ, Cowan A, Hyman MC, Rabinowitz JD, Frankel DS, Arany Z. Comprehensive quantification of fuel use by the failing and nonfailing human heart. *Science*. 2020;370(6514):364–8.
52. Ingalls AM, Dickie MM, Snell GD. Obese, a new mutation in the house mouse. *J Hered*. 1950;41(12):317–8.
53. Buchanan J, Mazumder PK, Hu P, Chakrabarti G, Roberts MW, Yun UJ, Cooksey RC, Litwin SE, Abel ED. Reduced cardiac efficiency and altered substrate metabolism precedes the onset of hyperglycemia and contractile dysfunction in two mouse models of insulin resistance and obesity. *Endocrinology*. 2005;146(12):5341–9.
54. Moellmann J, Klinkhammer BM, Droste P, Kappel B, Haj-Yehia E, Maxeiner S, Artati A, Adamski J, Boor P, Schutt K, et al. Empagliflozin improves left ventricular diastolic function of Db/db mice. *Biochim Biophys Acta Mol Basis Dis*. 2020;1866(8):165807.
55. Vanweert F, de Ligt M, Hoeks J, Hesselink MKC, Schrauwen P, Phielix E. Elevated plasma branched-chain amino acid levels correlate with type 2 diabetes-related metabolic disturbances. *J Clin Endocrinol Metab*. 2021;106(4):e1827–36.
56. Obayashi M, Shimomura Y, Nakai N, Jeoung NH, Nagasaki M, Murakami T, Sato Y, Harris RA. Estrogen controls branched-chain amino acid catabolism in female rats. *J Nutr*. 2004;134(10):2628–33.

Publisher's note

Springer Nature remains neutral with regard to jurisdictional claims in published maps and institutional affiliations.